

Disorder-induced critical phenomena in hysteresis: Numerical scaling in three and higher dimensions

Olga Perković,* Karin A. Dahmen,† and James P. Sethna

Laboratory of Atomic and Solid State Physics, Cornell University, Ithaca, New York 14853-2501

(Received 27 July 1998)

We present numerical simulations of avalanches and critical phenomena associated with hysteresis loops, modeled using the zero-temperature random-field Ising model. We study the transition between smooth hysteresis loops and loops with a sharp jump in the magnetization, as the disorder in our model is decreased. In a large region near the critical point, we find scaling and critical phenomena, which are well described by the results of an ϵ expansion about six dimensions. We present the results of simulations in three, four, and five dimensions, with systems with up to a billion spins (1000^3). [S0163-1829(99)03709-1]

I. INTRODUCTION

The increased interest in real materials in condensed-matter physics has brought disordered systems into the spotlight. Dirt changes the free-energy landscape of a system, and can introduce metastable states with large energy barriers.¹ This can lead to extremely slow relaxation towards the equilibrium state. On long length scales and practical time scales, a system driven by an external field will move from one metastable local free-energy minimum to the next. The equilibrium, global free-energy minimum and the thermal fluctuations that drive the system toward it, are in this case irrelevant. The state of the system will instead depend on its history.

The motion from one local minima to the next is a collective process involving many local (magnetic) domains in a local region—an *avalanche*. In magnetic materials, as the external magnetic field H is changed continuously, these avalanches lead to the magnetic noise: the Barkhausen effect.^{2,3} This effect can be picked up as voltage pulses in a coil surrounding the magnet. The distribution of pulse (avalanche) sizes is found³⁻⁶ to follow a power law with a cutoff after a few decades, and was interpreted by some⁶ to be an example of self-organized criticality (SOC).⁷ (In SOC, a system organizes itself into a critical state without the need to tune an external parameter.) Other systems can exhibit avalanches as well. Several examples where disorder may play a part are: superconducting vortex line avalanches,⁸ resistance avalanches in superconducting films,⁹ and capillary condensation of helium in Nuclepore.¹⁰

The history dependence of the state of the system leads to hysteresis. Experiments with magnetic tapes¹¹ have shown that the shape of the hysteresis curve changes with the annealing temperature. The hysteresis curve goes from smooth to discontinuous as the annealing temperature is increased. This transition can be explained in terms of a *plain old critical point* with two tunable parameters: the annealing temperature and the external field. At the critical temperature and field, the correlation length diverges, and the distribution of pulse (avalanche) sizes follows a power law.

We have argued earlier¹² that the Barkhausen noise ex-

periments can be quantitatively explained by a model¹³ with two tunable parameters (external field and disorder), which exhibits *universal*, nonequilibrium collective behavior. The model is athermal and incorporates collective behavior through nearest-neighbor interactions. The role of *dirt* or disorder, as we call it, is played by random fields. This paper presents the results and conclusions of a large scale simulation of that model: the nonequilibrium zero-temperature random field Ising model (RFIM), with a deterministic dynamics. The results compare very well to our ϵ expansion,^{14,15} and to experiments in Barkhausen noise.¹²

We should mention that there are other models for avalanches in disordered magnets. There is a large body of work on depinning transitions and the motion of the single interface.¹⁶⁻¹⁸ In these models, avalanches occur only at the growing interface. Our model though, deals with many interacting interfaces: avalanches can grow anywhere in the system. Models of hysteresis similar to ours exist,¹⁹ including ones with random bonds^{20,21} and random anisotropies.

This paper is a condensed version of an unpublished manuscript, available electronically.²² We focus here on the numerical results and scaling methods in dimensions three through six. Some of the other topics touched upon in the original manuscript are being published separately. Our interpretation of the behavior in dimension two has been substantially altered by further analysis.²³ A full description of the numerical method is available, including sample code and executables, on the World Wide Web.²⁴ For a full discussion of the behavior in mean field theory, and interesting behavior below the critical point in seven and nine dimensions, we refer the reader to the electronic version of the original manuscript,²² and to recent work on the Bethe lattice.²⁵

II. THE MODEL

The model we use is the zero-temperature random-field Ising model,^{19,16,13,12} which we briefly review here. Magnetic domains are represented by spins s_i on a hypercubic lattice, which can take two values: $s_i = \pm 1$. The spins interact ferromagnetically with their nearest neighbors with a strength

J_{ij} , and are exposed to a uniform magnetic field H (which is directed along the spins). Disorder is simulated by a random field h_i , associated with each site of the lattice, which is given by a Gaussian distribution function $\rho(h_i)$,

$$\rho(h_i) = \frac{1}{\sqrt{2\pi R}} e^{-h_i^2/2R^2}, \quad (1)$$

of width proportional to R , which we call the disorder. The Hamiltonian is then

$$\mathcal{H} = - \sum_{\langle i,j \rangle} J_{ij} s_i s_j - \sum_i (H + h_i) s_i. \quad (2)$$

For the analytic calculation, as well as the simulation, we have set the interaction between the spins to be independent of the spins and equal to one for nearest neighbors, $J_{ij} = J = 1$, and zero otherwise. We use periodic boundary conditions in the results of this paper; we've checked that the results near R_c are unchanged when a slab of preflipped spins is introduced (fixed boundary conditions along two sides).

The dynamics is deterministic, and is defined such that a spin s_i will flip only when its local effective field h_i^{eff} ,

$$h_i^{eff} = J \sum_j s_j + H + h_i, \quad (3)$$

changes sign. All the spins start pointing down ($s_i = -1$ for all i). As the field is adiabatically increased, a spin will flip. Due to the nearest-neighbor interaction, a flipped spin will push a neighbor to flip, which in turn might push another neighbor, and so on, thereby generating an avalanche of spin flips. During each avalanche, the external field is kept constant. For large disorders, the distribution of random fields is wide, and spins will tend to flip independently of each other. Only small avalanches will exist, and the magnetization curve will be smooth. On the other hand, a small disorder implies a narrow random-field distribution which allows larger avalanches to occur. As the disorder is lowered, at the disorder $R = R_c$ and field $H = H_c$, an infinite avalanche in the thermodynamic system will occur for the first time, and the magnetization curve will show a discontinuity. Near R_c and H_c , we find critical scaling behavior and avalanches of all sizes. Therefore, the system has two tunable parameters: the external field H and the disorder R . We found from the mean-field calculation^{13–15} and the simulation that a discontinuity in the magnetization exists for disorders $R \leq R_c$, at the field $H_c(R) \geq H_c(R_c)$, but that only at (R_c, H_c) , do we have critical behavior. For finite size systems of length L , the transition occurs at the disorder $R_c^{eff}(L)$ near which avalanches first begin to span the system in one of the d dimensions (spanning avalanches). The effective critical disorder $R_c^{eff}(L)$ is larger than R_c , and $R_c^{eff}(L) \rightarrow R_c$ as $L \rightarrow \infty$.

The algorithm we use to simulate this model is described in a separate manuscript.²⁴ For a simulation with N spins, the computer time scales as $N \log N$ and the memory required for the simulation scales to one bit per spin (i.e., we do not store the random fields).

III. SCALING

We use data obtained from the simulation to find and describe the critical transition. We do so using ‘‘scaling collapses,’’ which we review briefly here. For example, the magnetization as a function of external field H is expected to have the form

$$M(H, R) - M_c(H_c, R_c) \sim |r|^\beta \mathcal{M}_\pm(h'/|r|^{\beta\delta}), \quad (4)$$

where M_c is the critical magnetization (the magnetization at H_c , for $R = R_c$), $r = (R - R_c)/R$ and $h = (H - H_c)$ are the reduced disorder and reduced field, respectively,

$$h' = h + Br \quad (5)$$

is a (nonuniversal) rotation between the experimental control variables (r, h) and the scaling variables (r, h') , and \mathcal{M}_\pm is a universal scaling function (\pm refers to the sign of r). [In the plots shown in this paper, we use $r = (R - R_c)/R$, which we have found produces better collapses than using $r = (R - R_c)/R_c$. The latter is more traditional, but the two definitions agree as $R \rightarrow R_c$, and differ by an amount which is irrelevant in a renormalization-group sense. One method we use to estimate error in our exponents is to compare extrapolations based on the two definitions.] Scaling is expected asymptotically for small r and h —i.e., for H near H_c and R near R_c . The critical exponent β gives the scaling for the magnetization at the critical field H_c ($h = 0$). If we plot $|r|^{-\beta} (M(H, R) - M_c(H_c, R_c))$ versus $h/r^{\beta\delta}$, we should obtain the curve $\mathcal{M}(x)$, independently of what disorder R we choose (so long as it is close to R_c): different experimental and numerical data sets should collapse onto one universal curve $\mathcal{M}(x)$. (Actually, one has two curves \mathcal{M}_\pm depending on whether $R > R_c$ or $R < R_c$.) We use scaling forms similar to Eq. (4) to analyze all of our measurements.

One can easily show using the scaling form (4) that the magnetization scales with a power law $M - M_c \sim h^\delta$ at R_c , and that the jump in the magnetization (the size of the infinite avalanche) scales as $\Delta M \sim r^\beta$ as one varies the disorder below R_c . Thus the critical exponents β and δ give the power laws for the singularities in these measured quantities: indeed, that is how these exponents were originally defined and measured. In our system, we will find that directly measuring power laws is not effective in getting good exponents: the critical regime is so large that we need both to use the general scaling form and to extrapolate to the critical point.

The explanatory power of the theory resides in the fact that the same universal critical exponents β and δ and the same universal function $\mathcal{M}(x)$ should be obtained by simulations at different values of the disorder, simulations of different Hamiltonians, and simulations of real experiments, so long as the systems share certain important features and symmetries (so long as they lie in the same universality class). The underlying explanation for why universality and scaling should occur near the critical point is given by the renormalization group.^{26,14,15,22} Above six dimensions, fluctuations are asymptotically not important, and we can calculate $\mathcal{M}(x)$ and the values of β and δ from mean-field theory ($\beta_{MF} = 1/2$, $\delta_{MF} = 3$).¹³ Below six dimensions, the exponents and scaling curves are nontrivial, and to find them one must rely on either perturbative methods,^{14,15} experiments, or numerical methods^{13,22} as used here.

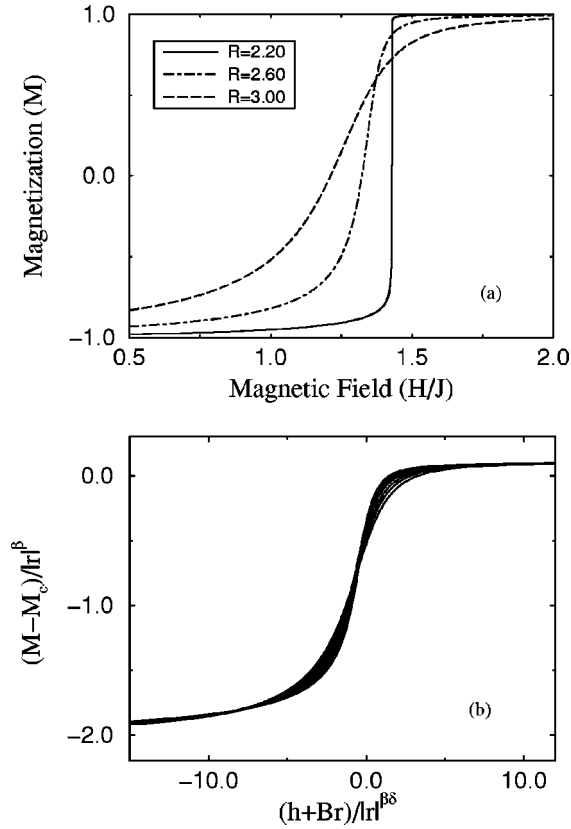


FIG. 1. (a) Magnetization curves in three dimensions for size $L=320$, and three values of disorder. The curves are averages of up to 48 different random-field configurations. Note the discontinuity in the magnetization for $R=2.20$. In finite size systems, the discontinuity in the magnetization curve occurs even for $R > R_c$ ($R_c = 2.16$ in three dimensions). (b) Scaling collapse (see text) of the magnetization curves in three dimensions for size $L=320$. The disorders range from $R=2.35$ to $R=3.20$. The critical magnetization is chosen as $M_c=0.9$ from an analysis of the magnetization curves and is kept fixed during the collapse. The universal exponents are $\beta=0.036$, $\beta\delta=1.81$. The nonuniversal critical field $H_c=1.435$, critical disorder $R_c=2.16$, and rotation parameter $B=0.39$.

IV. THE SIMULATION RESULTS

The following measurements were obtained from the simulation as a function of disorder R : the magnetization $M(H, R)$ as a function of the external field H ; the avalanche size distribution integrated over the field $H: D_{int}(S, R)$; the avalanche correlation function integrated over the field $H: G_{int}(x, R)$; the number of spanning avalanches $N(L, R)$ as a function of the system length L , integrated over the field H ; the discontinuity in the magnetization $\Delta M(L, R)$ as a function of the system length L ; the second $\langle S^2 \rangle_{int}(L, R)$, third $\langle S^3 \rangle_{int}(L, R)$, and fourth $\langle S^4 \rangle_{int}(L, R)$ moments of the avalanche size distribution as a function of the system length L , integrated over the field H . In addition, we have measured: the avalanche size distribution $D(S, H, R)$ as a function of the field H and disorder R ; the distribution of avalanche times $D_t^{(int)}(S, t)$ as a function of the avalanche size S , at $R = R_c$, integrated over the field H .

We do not present results on the sample-to-sample fluctuations in these systems, which would themselves have had interesting scaling properties:^{27,28} at the critical point, fluc-

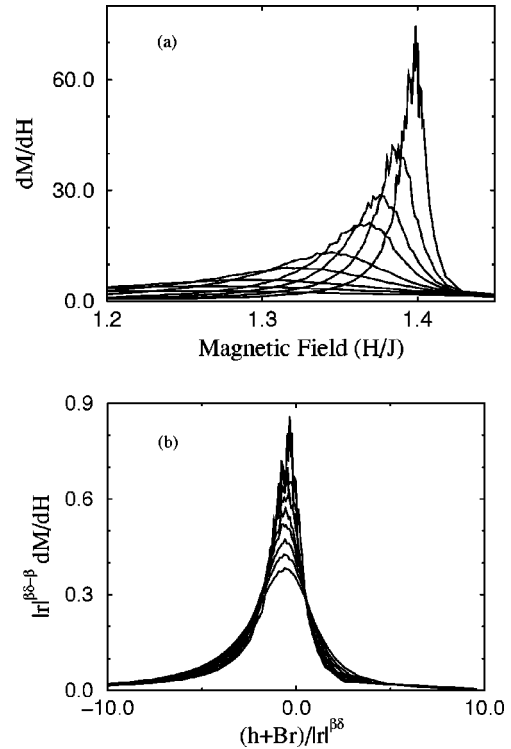


FIG. 2. dM/dH curves in three dimensions. (a) Derivative of the magnetization M with respect to the field H for disorders $R = 2.35, 2.4, 2.45, 2.5, 2.6, 2.7, 2.85, 3.0$, and 3.2 (highest to lowest peak), (b) Scaling collapse of the data in (a) with $\beta = 0.036$, $\beta\delta = 1.81$, $B = 0.39$, $H_c = 1.435$, and $R_c = 2.16$. While the curves are not collapsing onto a single curve, the quality of the collapse is quite similar to that found at similar distances from R_c in mean-field theory,²² for which we know analytically that scaling works as $R \rightarrow R_c$.

tuations in disordered systems often persist even in the limit of infinite system size (lack of self-averaging). There has also been recent interest in the distinction in finite-size simulations between scaling collapses using the average value of the critical point versus scaling while allowing the effective critical point to fluctuate between systems. In some systems scaling collapses with effective, sample dependent critical points can converge substantially faster;²⁸ in some systems it has been suggested that new critical exponents can be revealed;²⁹ and in one system an unusual new regime of large fluctuations was revealed.³⁰ Our major obstacle to good collapses and exponents was getting close to the critical disorder (demanding huge simulations to encompass the resulting avalanches), not in extracting average behavior from the fluctuations. A future study of the fluctuations in the measured properties in this system would be worthwhile.

A. Magnetization curves

Unfortunately the most obvious measured quantity in our simulations, the magnetization curve $M(H)$, is the one which collapses least well in our simulations. We start with it nonetheless.

Figure 1(a) shows the magnetization curves obtained from our simulation in three dimensions for several values of the disorder R . As the disorder R is decreased, a discontinuity or jump in the magnetization curve appears where a single ava-

TABLE I. Universal critical exponents. Values for the exponents extracted from scaling collapses in three, four, and five dimensions. The mean-field values are calculated analytically.^{13,14} ν is the correlation length exponent and is found from collapses of avalanche correlations, number of spanning avalanches, and moments of the avalanche size distribution data. The exponent θ is a measure of the number of spanning avalanches and is obtained from collapses of those data. $(\tau + \sigma\beta\delta - 3)/\sigma\nu$ is obtained from the second moments of the avalanche size distribution collapses. $1/\sigma$ is associated with the cutoff in the power-law distribution of avalanche sizes integrated over the field H , while $\tau + \sigma\beta\delta$ gives the slope of that distribution. τ is obtained from the binned avalanche size distribution collapses. $d + \beta/\nu$ is obtained from avalanche correlation collapses and β/ν from magnetization discontinuity collapses. $\sigma\nu z$ is the exponent combination for the time distribution of avalanche sizes and is extracted from those data. Error bars are based on variations in the results based on different approaches to the analysis: statistical fluctuations are typically smaller.

Measured exponents	3d	4d	5d	Mean field
$1/\nu$	0.71 ± 0.09	1.12 ± 0.11	1.47 ± 0.15	2
θ	0.015 ± 0.015	0.32 ± 0.06	1.03 ± 0.10	1
$(\tau + \sigma\beta\delta - 3)/\sigma\nu$	-2.90 ± 0.16	-3.20 ± 0.24	-2.95 ± 0.13	-3
$1/\sigma$	4.2 ± 0.3	3.20 ± 0.25	2.35 ± 0.25	2
$\tau + \sigma\beta\delta$	2.03 ± 0.03	2.07 ± 0.03	2.15 ± 0.04	9/4
τ	1.60 ± 0.06	1.53 ± 0.08	1.48 ± 0.10	3/2
$d + \beta/\nu$	3.07 ± 0.30	4.15 ± 0.20	5.1 ± 0.4	7 (at $d_c = 6$)
β/ν	0.025 ± 0.020	0.19 ± 0.05	0.37 ± 0.08	1
$\sigma\nu z$	0.57 ± 0.03	0.56 ± 0.03	0.545 ± 0.025	1/2

lanche occupies a large fraction of the total system. In the thermodynamic limit this would be the infinite avalanche: the largest disorder at which it occurs is the critical disorder R_c . For finite size systems, like the ones we use in our simulation, we observe an avalanche which spans the system at a higher disorder, which gradually approaches R_c as the system size grows.

Figure 2 shows the slope dM/dH and its scaling collapse. By using this derivative, the critical region is emphasized as the peak in the curve, and the dependence on the parameter M_c drops out. The lower graphs in Figs. 1(b) and 2(b) show the scaling collapses of the magnetization and its slope. Clearly in neither case are all the data collapsing onto a single curve. This would be distressing, were it not for the fact that this also occurs in mean-field theory²² at a similar distance to the critical point.

Because the scaling of the magnetization is so bad, we use other quantities to estimate the critical exponents and the location of the critical point (Tables I and II). Fixing these quantities, we use the collapse of the dM/dH curves to extract the rotation B mixing the experimental variables r and h into the scaling variable $h' = h + Br$ [Eq. (5)].

B. Avalanche size distribution

1. Integrated avalanche size distribution

In our model the spins flip in avalanches: each spin can kick over one or more neighbors in a cascade. These avalanches come in different sizes. The integrated avalanche size distribution is the size distribution of all the avalanches that occur in one branch of the hysteresis loop (for H from $-\infty$ to ∞). Figure 3 (Ref. 12) shows some of the raw data (thick lines) in three dimensions. Note that the curves follow an approximate power-law behavior over several decades. Even 50% away from criticality (at $R = 3.2$), there are still two decades of scaling, which implies that the critical region is large. In experiments, a few decades of scaling could be interpreted in terms of self-organized criticality (SOC). However, our model and simulation suggest that several decades of power-law scaling can still be present rather *far* from the critical point (note that the size of the critical region is non-universal). The slope of the log-log avalanche size distribution at R_c gives the critical exponent $\tau + \sigma\beta\delta$. Notice, however, that the apparent slopes in Fig. 3 continue to change even after several decades of apparent scaling is obtained.

TABLE II. Nonuniversal scaling variables. Numerical values for the critical disorders and fields, and the rotation parameter B [Eq. (5)], in three, four, and five dimensions extracted from scaling collapses. The critical disorder is obtained from collapses of the spanning avalanches and the second moments of the avalanche size distribution. The critical field is obtained from the binned avalanche size distribution and the magnetization curves. H_c is affected by finite sizes, and systematic errors could be larger than the ones listed here. The mean-field values are calculated analytically.^{13,14} The rotation B is obtained from the dM/dH collapses.

	3d	4d	5d	Mean field
R_c	2.16 ± 0.03	4.10 ± 0.02	5.96 ± 0.02	0.79788456
H_c	1.435 ± 0.004	1.265 ± 0.007	1.175 ± 0.004	0
B	0.39 ± 0.08	0.46 ± 0.05	0.23 ± 0.08	0

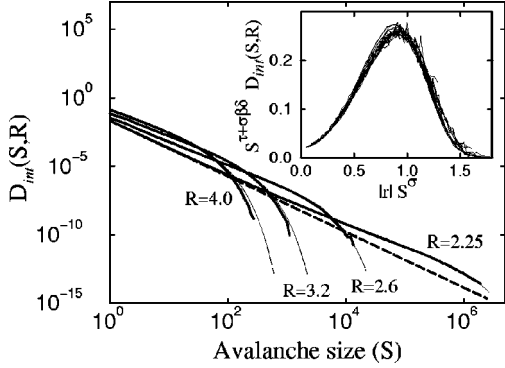


FIG. 3. Integrated avalanche size distribution curves in three dimensions for 320^3 spins and disorders $R=4.0, 3.2,$ and 2.6 . The last curve is at $R=2.25$, for a 1000^3 spin system. The 320^3 curves are averages over up to 16 initial random-field configurations. The inset shows the scaling collapse of the integrated avalanche size distribution curves in three dimensions, using $r=(R-R_c)/R$, $\tau+\sigma\beta\delta=2.03$, and $\sigma=0.24$, for sizes $160^3, 320^3, 800^3,$ and 1000^3 , and disorders ranging from $R=2.25$ to $R=3.2$ ($R_c=2.16$). The two top curves in the collapse, at $R=3.2$, show noticeable corrections to scaling. The thick dark curve through the collapse is the fit to the data (see text). In the main figure, the distribution curves obtained from the fit to the collapsed data are plotted (thin lines) alongside the raw data (thick lines). The straight dashed line is the expected asymptotic power-law behavior: $S^{-2.03}$, which does not agree with the measured slope of the raw data due to the shape of the scaling function (see text).

The cutoff in the power law diverges as the critical disorder R_c is approached. This cutoff size scales as $S\sim|r|^{-1/\sigma}$.

These critical exponents can be obtained by using a scaling collapse for the curves of Fig. 3, shown in the inset. The scaling form is

$$D_{int}(S,R)\sim S^{-(\tau+\sigma\beta\delta)}\bar{D}_+^{(int)}(S^\sigma|r|), \quad (6)$$

where $\bar{D}_+^{(int)}$ is the scaling function (the + sign indicates that the collapsed curves are for $R>R_c$). We are sufficiently far from the critical point that corrections to scaling are important: as described in Ref. 22, we do collapses for small ranges of R and then linearly extrapolate the best-fit critical exponents to R_c . We estimate from this curve that the critical exponents $\tau+\sigma\beta\delta=2.03$ and $\sigma=0.24$.

The scaling function $\bar{D}_+^{(int)}(X)$ with $X=S^\sigma|r|$ is a universal prediction of our model. To facilitate comparisons with experiments, we fit a curve to the data collapse in the inset of Fig. 3. We have fit the scaling collapses in dimensions three, four, and five to a phenomenological form of an exponential times a polynomial. In three dimensions, our fit is

$$\bar{D}_+^{(int)}(X)=e^{-0.789X^{1/\sigma}}\times(0.021+0.002X+0.531X^2-0.266X^3+0.261X^4), \quad (7)$$

where $1/\sigma=4.20$. The distribution curves obtained using the above fit are plotted (thin lines in Fig. 3) alongside the raw data (thick lines). They agree remarkably well even far above R_c . We should recall though, that the fitted curve to the collapsed data can differ from the ‘‘real’’ scaling function even for large sizes and close to the critical disorder (in mean field²² the error in the corresponding curve was about 10%).

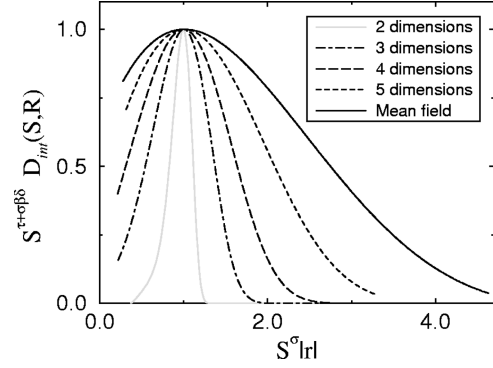


FIG. 4. Integrated avalanche size distribution scaling functions in two, three, four, and five dimensions, and mean field. The curves are fits (see text) to the scaling collapses done with exponents from Table I and corresponding calculations in two dimensions.²³ The peaks are aligned to fall on (1,1). Due to the ‘‘bump’’ in the scaling function the power-law exponent can not be extracted from a linear fit to the raw data for reasonable simulation sizes.¹²

The scaling function in the inset of Fig. 3 has a peculiar shape: it grows by a factor of 10 before cutting off. The consequence of this bump in the shape is that in the simulations it takes many decades in the size distribution for the slope to converge to the asymptotic power law. This can be seen from the comparison between a straight line fit through the $R=2.25$ (billion spin) simulation in Fig. 3 and the asymptotic power law $S^{-2.03}$ obtained from extrapolating the scaling collapses (thick dashed straight line in the same figure). A similar bump exists in other dimensions and mean field as well. Figure 4 shows the scaling functions in different dimensions and in mean field. In this graph, the scaling functions are normalized to one and the peaks are aligned (the scaling forms allow this). The curves plotted in Fig. 4 are not raw data but fits to the scaling collapse in each dimension, as was done in the inset of Fig. 3. For five, four, and three dimensions, we have, respectively:

$$\bar{D}_5^{(int)}(X)=e^{-0.518X^{1/\sigma}}\times(0.112+0.459X-0.260X^2+0.201X^3-0.050X^4), \quad (8)$$

$$\bar{D}_4^{(int)}(X)=e^{-0.954X^{1/\sigma}}\times(0.058+0.396X+0.248X^2-0.140X^3+0.026X^4), \quad (9)$$

$$\bar{D}_2^{(int)}(X)=e^{-1.076X^{1/\sigma}}\times(0.492-4.472X+14.702X^2-20.936X^3+11.303X^4), \quad (10)$$

with $1/\sigma=2.35, 3.20,$ and 10.0 . The errors in the fits are again in the 10% range, judging from mean-field theory.²²

In mean-field theory (dimensions six and greater) a similar fit²² to the analytical form of the scaling function above R_c gives

$$\bar{D}_{MF}^{(int)}(X)=e^{-X^2/2}(0.204+0.482X-0.391X^2+0.204X^3-0.048X^4). \quad (11)$$

It is clear from the figure that the growing bump in the scaling curves as the dimension decreases is a foreshadowing of a zero in the scaling curve in two dimensions: this will be discussed further in Ref. 23.

2. Binned in H avalanche size distribution

The avalanche size distribution can also be measured at a field H or in a small range of fields centered around H . We have measured this binned in H avalanche size distribution for systems at the critical disorder R_c ($r=0$). To obtain the scaling form, we start from the distribution of avalanches at field H and disorder R :

$$D(S,R,H) \sim S^{-\tau} \mathcal{D}_{\pm}(S^{\sigma}|r'|, |h|/|r'|^{\beta\delta}), \quad (12)$$

where as before \mathcal{D}_{\pm} is the scaling function and \pm indicates the sign of r .

The parameter B of Eq. (5), which rotates the measured axes (r,h) into the scaling axes $(r,h'=h+Br)$, will be important²² only for large avalanches of size $S > h^{-1/\sigma}$ near the critical point. In three and four dimensions, this does not affect our scaling collapses; in five dimensions we account for it.²²

The scaling function can be rewritten as $\hat{\mathcal{D}}_{\pm}(S^{\sigma}|r|, (S^{\sigma}|r|)^{\beta\delta}|h|/|r|^{\beta\delta})$, where $\hat{\mathcal{D}}_{\pm}$ is a new scaling function and \pm represents whether H is greater than or less than H_c (i.e., H rather than R). Letting $R \rightarrow R_c$, the scaling for the avalanche size distribution at the field H , measured at the critical disorder R_c is:

$$D(S,H) \sim S^{-\tau} \hat{\mathcal{D}}_{\pm}(|h|S^{\sigma\beta\delta}). \quad (13)$$

Figure 5(a) shows the binned in H avalanche size distribution curves in four dimensions, for values of H below the critical field H_c . (The curves and analysis are similar in three and five dimensions; results in four dimensions are used here for variety.) The simulation was done at the best estimate of the critical disorder R_c (4.1 in four dimensions). The binning in H is logarithmic and started from an approximate critical field H_c obtained from the magnetization curves; better estimates of H_c are then obtained from the binned distribution data curves and their collapses. Our best estimate for the critical field H_c in four dimensions is 1.265 ± 0.007 . The scaling form for the logarithmically binned data is the same as in Eq. (13), if the log-binned data is normalized by the size of the bin. Figure 5(b) shows the scaling collapse for our data, both below and above the critical field H_c . The ‘‘top’’ collapse gives the shape of the $\hat{\mathcal{D}}_{-}$ ($H < H_c$) function, while the ‘‘bottom’’ collapse gives the $\hat{\mathcal{D}}_{+}$ ($H > H_c$) function. Above the critical field H_c , there are spanning avalanches in the system.³¹ These are not included in the binned avalanche size distribution collapse shown in Fig. 5(b).

The exponent τ which gives the power-law behavior of the binned avalanche size distribution is obtained from collapses of neighboring curves as described above,²² extrapolating to $H=H_c$. The exponent $\sigma\beta\delta$ is found to be very sensitive to H_c , while τ is not. We have therefore used the values of $\tau + \sigma\beta\delta$ and σ from the integrated avalanche size distribution collapses, and τ from the binned avalanche size distribution collapses to further constrain H_c (by constrain-

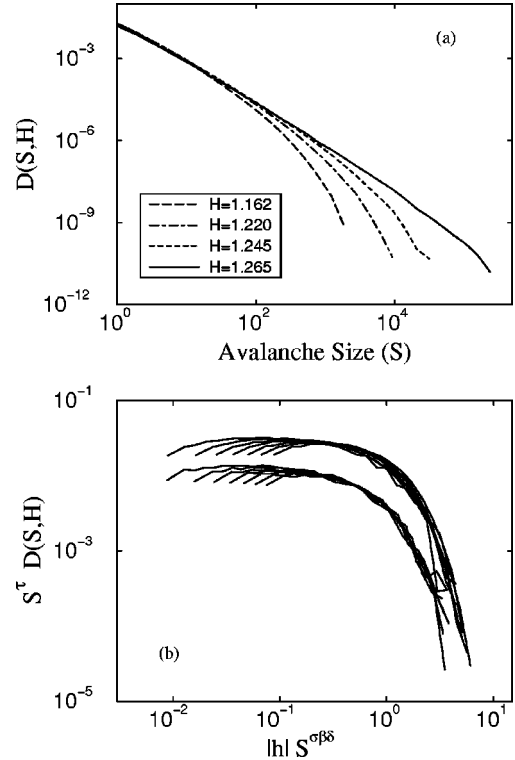


FIG. 5. (a) Binned in H avalanche size distribution in four dimensions for a system of 80^4 spins at $R=4.09$ ($R_c=4.10$). The critical field is $H_c=1.265$. The curves are averages over close to 60 random-field configuration. Only a few curves are shown. (b) Scaling collapse of the binned avalanche size distribution for $H < H_c$ (upper collapse) and $H > H_c$ (lower collapse). The critical exponents are $\tau=1.53$ and $\sigma\beta\delta=0.54$, and the critical field is $H_c=1.265$. The bins are at fields 1.162, 1.185, 1.204, 1.220, 1.234, 1.245, 1.254, 1.276, 1.285, 1.296, 1.310, 1.326, 1.345, and 1.368.

ing $\sigma\beta\delta$), and to calculate $\beta\delta$. The latter is then used to obtain collapses of the magnetization curves. We should mention here that H_c in all the dimensions is difficult to find and that it is influenced by finite sizes. The values listed in Table II are the best estimates obtained from the largest system sizes we have. Nevertheless, systematic errors for H_c could be larger than the errors given in Table II. These errors could produce systematic errors for $\sigma\beta\delta$ which depends on H_c , and for $\beta\delta$ which is calculated from $\sigma\beta\delta$: hence errors in these exponents could also be larger than the errors listed in Table III.

From Fig 5(b), we see that the two-binned avalanche size distribution scaling function does not have a ‘‘bump’’ as does the scaling function for the integrated avalanche size distribution (inset in Fig. 3). Therefore we expect that the exponent τ which gives the slope of the distribution in Fig. 5(a) can also be obtained by a linear fit through the data curve closest to the critical field. Figure 6 shows the curve for the $H=1.265$ bin (dashed curve) as well as the linear fit. The slope from the linear fit is 1.55 while the value of τ obtained from the collapses and the extrapolation in Fig. 5 is 1.53 ± 0.08 .

C. Avalanche correlations

The avalanche correlation function $G(x,R,H)$ measures the probability that the initial spin of an avalanche will trig-

TABLE III. Values for exponents in three, four, and five dimensions that are not extracted directly from scaling collapses, but instead are derived from Table I and the exponent relations (see Ref. 14). The mean-field values are obtained analytically.^{13,14} Both $\sigma\beta\delta$ and $\beta\delta$ could have larger systematic errors than the errors listed here. See the binned avalanche size distribution section for details.

Calculated exponents	3d	4d	5d	Mean field
$\sigma\beta\delta$	0.43 ± 0.07	0.54 ± 0.08	0.67 ± 0.11	3/4
$\beta\delta$	1.81 ± 0.32	1.73 ± 0.29	1.57 ± 0.31	3/2
β	0.035 ± 0.028	0.169 ± 0.048	0.252 ± 0.060	1/2
$\sigma\nu$	0.34 ± 0.05	0.28 ± 0.04	0.29 ± 0.04	1/4
$\eta = 2 + (\beta - \beta\delta)/\nu$	0.73 ± 0.28	0.25 ± 0.38	0.06 ± 0.51	0

ger, in that avalanche, another spin a distance x away. From the renormalization-group description,^{14,15} close to the critical point and for large distances x , the correlation function is given by

$$G(x, R, H) \sim \frac{1}{x^{d-2+\eta}} \mathcal{G}_{\pm}[x/\xi(r, h)], \quad (14)$$

where r and h are, respectively, the reduced disorder and field, \mathcal{G}_{\pm} (\pm indicates the sign of r) is the scaling function, d is the dimension, ξ is the correlation length, and η is called the ‘‘anomalous dimension.’’ Corrections can be shown to be subdominant.²² The correlation length $\xi(r, h)$ is a macroscopic length scale in the system which is on the order of the mean linear extent of the largest avalanches. At the critical field H_c ($h=0$) and near R_c , the correlation length scales like $\xi \sim |r|^{-\nu}$, while for small field h it is given by

$$\xi \sim |r|^{-\nu} \mathcal{Y}_{\pm}(h/|r|^{\beta\delta}), \quad (15)$$

where \mathcal{Y}_{\pm} is a universal scaling function. The avalanche correlation function should not be confused with the cluster or ‘‘spin-spin’’ correlation which measures the probability that two spins a distance x away have the same value. (The algebraic decay for this other, spin-spin correlation function at the critical point ($r=0$ and $h=0$), is $1/x^{d-4+\tilde{\eta}}$.¹⁴)

We’ve mostly used, for historical reasons, a slightly different avalanche correlation function, which scales the same way as the ‘‘triggered’’ correlation function G described

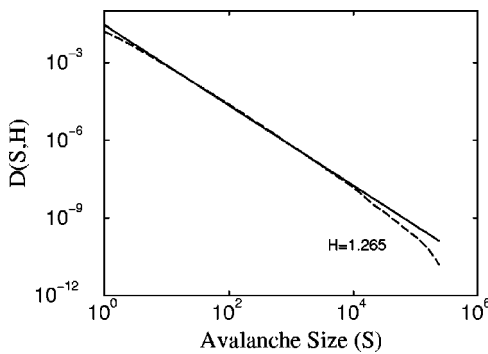


FIG. 6. Linear fit to binned avalanche size distribution curve in four dimensions, for a system of 80^4 spins at $R_c = 4.09$. The magnetic field is $H = 1.265$. The straight solid line is a linear fit to the data for $S < 13,000$ spins. The slope from the fit is 1.55 (this varies by not more than 3% as the range over which the fit is done is changed), while the exponent τ obtained from the collapses and the extrapolation in Fig. 5 is 1.53 ± 0.08 .

above. Our function basically ignores the difference between the triggering spin and the other spins in the avalanche: alternatively, it calculates for avalanches of size S the correlation function for pairs of spins, and then averages over all avalanches (weighting each avalanche equally). We’ve checked that our correlation function agrees to within 3% with the ‘‘triggered’’ correlation function described above, for $R > R_c$ in three dimensions and above. (In two dimensions, the two definitions differ more substantially, but appear to scale in the same way.²³)

We have measured the avalanche correlation function integrated over the field H , for $R > R_c$. For every avalanche that occurs between $H = -\infty$ and $H = +\infty$, we keep a count on the number of times a distance x occurs in the avalanche. To decrease the computational time not every pair of spins is selected; instead we do a statistical sampling. The spanning avalanches are not included in our correlation measurement. Figure 7 shows several avalanche correlation curves in three dimensions for $L = 320$. The scaling form for the avalanche correlation function integrated over the field H , close to the critical point and for large distances x , is obtained by integrating Eq. (14):

$$G_{int}(x, R) \sim \int \frac{1}{x^{d-2+\eta}} \mathcal{G}_{\pm}[x/\xi(r, h)] dh. \quad (16)$$

Using Eq. (15) and defining $u = h/|r|^{\beta\delta}$, Eq. (16) becomes

$$G_{int}(x, R) \sim |r|^{\beta\delta} x^{-(d-2+\eta)} \int \mathcal{G}_{\pm}[x/|r|^{-\nu} \mathcal{Y}_{\pm}(u)] du. \quad (17)$$

The integral (\mathcal{I}) in Eq. (17) is a function of $x/|r|^{\nu}$ and can be written as:

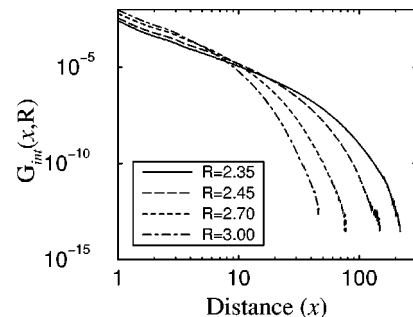


FIG. 7. Avalanche correlation function integrated over the field H in three dimensions, for $L = 320$. The curves are averages of up to 19 random-field configurations. The critical disorder R_c is 2.16.

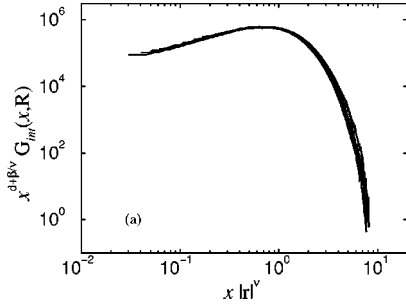


FIG. 8. Scaling collapse of the avalanche correlation function integrated over the field H , in three dimensions for $L=320$. The values of the disorders range from $R=2.35$ to $R=3.0$, with $R_c=2.16$. The exponents used in the collapse are $\nu=1.39\pm 0.20$ and $d+\beta/\nu=3.07\pm 0.30$. When collapses of neighboring curves are extrapolated to R_c , we get a slightly smaller value of $\nu=1.37\pm 0.18$.

$$\mathcal{I}=(x|r|^\nu)^{-\beta\delta/\nu}\tilde{\mathcal{G}}_\pm(x|r|^\nu) \quad (18)$$

to obtain the scaling form

$$G_{int}(x, R)\sim \frac{1}{x^{d+\beta/\nu}}\tilde{\mathcal{G}}_\pm(x|r|^\nu), \quad (19)$$

where we have used the scaling relation $(2-\eta)\nu=\beta\delta-\beta$ (see Ref. 14 for the derivation).

Figure 8 shows the integrated avalanche correlation curves collapse in three dimensions for $L=320$ and $R>R_c$. The exponent ν is obtained from such collapses by extrapolating to $R=R_c$ as was done for other collapses.²² The exponent β/ν can be obtained from these collapses too, but it is much better estimated from the magnetization discontinuity covered below. The value of β/ν listed in Table I is derived exclusively from the magnetization discontinuity collapses.

We have also looked for possible anisotropies in the integrated avalanche correlation function in two and three dimensions. The anisotropic integrated avalanche correlation functions are measured along ‘‘generalized diagonals’’: one along the three axis, the second along the six face diagonals, and the third along the four-body diagonals. We compare the integrated avalanche correlation function and the anisotropic integrated avalanche correlation functions to each other, and find no anisotropies in the correlation, as can be seen from Fig. 9.

D. Spanning avalanches

The critical disorder R_c was defined earlier as the disorder R at which an *infinite* avalanche first appears in the system, in the thermodynamic limit, as the disorder is lowered. At that point, the magnetization curve will show a discontinuity at the magnetization $M_c(R_c)$ and field $H_c(R_c)$. For each disorder R below the critical disorder, there is *one* infinite avalanche that occurs at a critical field $H_c(R)>H_c(R_c)$,^{14,15} while above R_c there are only finite avalanches. This is the behavior for an infinite-size system. In a finite-size system far below and above R_c the above picture is still true, but close to the critical disorder, as we approach the transition, the avalanches get larger and larger, and there will be a first

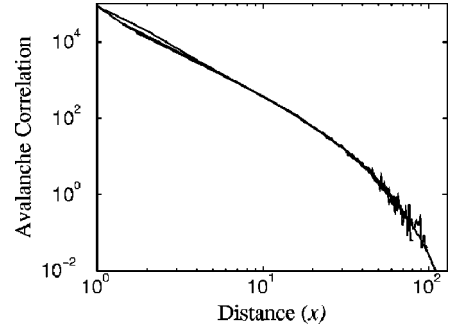


FIG. 9. Anisotropies in the avalanche correlation function. The curves are for a system of 320^3 spins at $R=2.35$. Four curves are shown on the graph: one is the avalanche correlation function integrated over the field H (as in Fig. 7), while the other three are measurements of the correlation along the three axis, the six face diagonals, and the four-body diagonals. Avalanches involving more than four spins show no noticeable anisotropy: the critical point appears to have spherical symmetry. The same result is found in two dimensions.

point where one of them will span the system from one side to another in at least one direction. This avalanche is not the infinite avalanche; if the system was larger, this avalanche would typically be nonsystem spanning. Such an avalanche (which spans the system) we call a spanning avalanche.

In our numerical simulation, we find that for finite sizes L , there are not one but *many* such avalanches in four and five dimensions (and maybe three), and that their number increases as the system size increases.³² Figures 10(a)–10(c) show the number of spanning avalanches as a function of disorder R , for different sizes and dimensions. In four and five dimensions, the spanning avalanche curves become more narrow as the system size is increased. Also, the peaks shift toward the critical value of the disorder (4.1 and 5.96, respectively), and the number of spanning avalanches at R_c increases. This suggests that in four and five dimensions, for $L\rightarrow\infty$, there will be one infinite avalanche below R_c , none above, and an infinite number of infinite, spanning avalanches at the critical disorder R_c . In three dimensions, the results are not conclusive, as noted both from Fig. 10(a) and from the value of the spanning avalanche exponent $\theta=0.15\pm 0.15$ defined below: a value of $\theta=0$ is consistent with one infinite or spanning avalanche at R_c as $L\rightarrow\infty$. It is clear that $\theta=0$ in two dimensions, since spanning avalanches can’t interpenetrate: it’s thus plausible that θ is near zero in three dimensions because it must vanish one dimension lower.

In percolation, a similar multiplicity of infinite clusters^{33,34} as the system size is increased is found for dimensions above six which is the upper critical dimension (UCD). The UCD is the dimension at and above which the mean-field exponents are valid. Below six dimensions, there is only one such infinite cluster in percolation. The existence of a diverging number of infinite clusters in percolation is associated with the breakdown of the hyperscaling relation above six dimensions. Since a hyperscaling relation is a relation between critical exponents that includes the dimension d of the system, it is always only satisfied up to and including the upper critical dimension. In our system, the upper critical dimension is also 6, but we find spanning avalanches in dimensions even below that. In a comment by Maritan

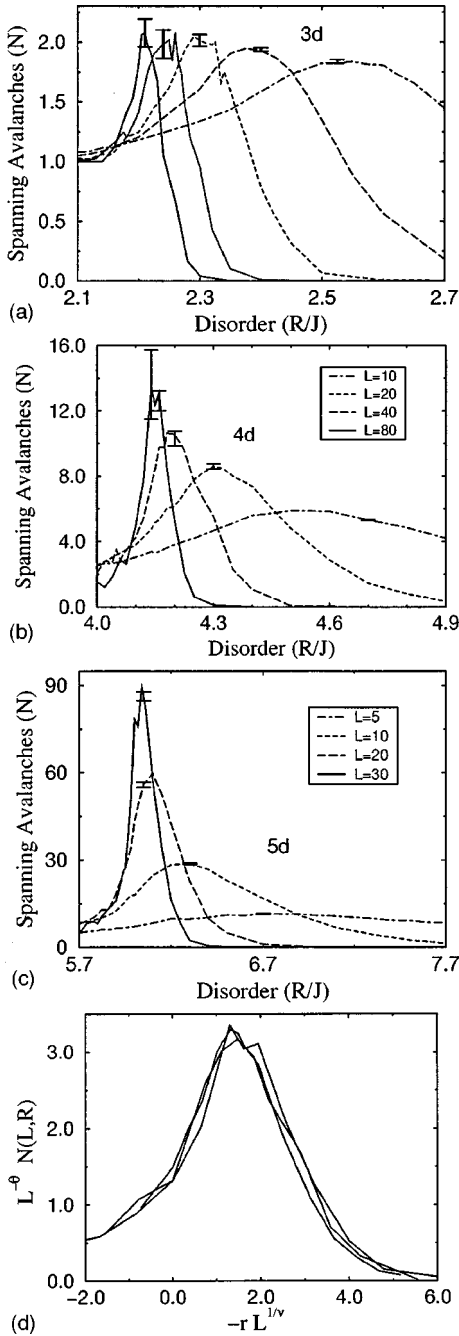


FIG. 10. Spanning avalanches in three, four, and five dimensions. (a) Number of spanning avalanches N in three dimensions, occurring in the system between $H = -\infty$ to $H = \infty$, as a function of the disorder R , for linear sizes L : 20 (dot-dashed), 40 (long dashed), 80 (dashed), 160 (dotted), and 320 (solid). The critical disorder R_c is at 2.16. The error bars for each curve tend to be smaller than the error bar shown at the peak for disorders above the peak and larger for disorders below the peak. They are not given here for clarity. Note that the number of avalanches increases only slightly as the size is increased. (b) Number of spanning avalanches in four dimensions. The critical disorder is 4.1. (c) Number of spanning avalanches in five dimensions. The critical disorder is 5.96. Both in four and five dimensions, the peaks grow and shift towards R_c as the size of the system is increased. (d) Collapse of the spanning avalanche curves in four dimensions for linear sizes $L = 20, 40, 80$. The exponents are $\theta = 0.32$ and $\nu = 0.89$, and the critical disorder is $R_c = 4.10$. The collapse is done using $r = (R_c - R)/R$.

et al.,³² it was suggested that our system should satisfy the hyperscaling relation $d\nu - \beta = 1/\sigma$ found in percolation.³⁴ But since our system has spanning avalanches below the upper critical dimension, this hyperscaling relation breaks down below six dimensions. Due to the existence of many spanning avalanches near R_c , the new “violation of hyperscaling” relation for dimensions three and above becomes¹⁴

$$(d - \theta)\nu - \beta = 1/\sigma, \quad (20)$$

where θ is the “breakdown of hyperscaling” or spanning avalanches exponent defined below. One can check that our exponents in three, four, and five dimensions and mean field satisfy this equation (see Tables I and III).

For the simulation, we define a spanning avalanche to be an avalanche that spans the system in a particular direction. We average over all the directions to obtain better statistics. Depending on the size and dimension of the system and the distance from the critical disorder, the number of spanning avalanches for a particular value of disorder R is obtained by averaging over as few as 5 to as many as 2000 different random-field configurations. We define the exponent θ such that the number N of spanning avalanches, at the critical disorder R_c , increases with the linear system size as: $N \sim L^\theta$ ($\theta > 0$). The finite-size scaling form³⁵ for the number of spanning avalanches close to the critical disorder is

$$N(L, R) \sim L^\theta \mathcal{N}_\pm(L^{1/\nu}|r|), \quad (21)$$

where ν is the correlation length exponent and \mathcal{N}_\pm is the corresponding scaling function (\pm indicates the sign of r). The collapse is shown in Fig. 10(d). (We show the collapses in four dimensions here since the existence of spanning avalanches in three dimensions is not conclusive.) These values are used along with the results from other collapses to obtain Table I. In the analysis of the avalanche size distribution, magnetization, and correlation functions for $R > R_c$, how close we chose to come to the critical disorder R_c was determined by the spanning avalanches: we include no values R below the first value which exhibited a spanning avalanche.

E. Magnetization discontinuity

We have mentioned earlier that in the thermodynamic limit, at and below the critical disorder R_c , there is a critical field $H_c(R) > H_c(R_c)$ at which the infinite avalanche occurs. Close to the critical transition, for small $r < 0$, the change in the magnetization due to the infinite avalanche scales as [Eq. (4)]

$$\Delta M(R) \sim r^\beta, \quad (22)$$

where $r = (R_c - R)/R$, while above the transition, there is no infinite avalanche.

In finite-size systems, the transition is not as sharp: we have spanning avalanches above the critical disorder. If we measure the change in the magnetization due to all the spanning avalanches as a function of disorder R at various system sizes L , we expect it will obey finite-size scaling (as did the number of spanning avalanches):

$$\Delta M(L, R) \sim |r|^\beta \Delta \mathcal{M}_\pm(L^{1/\nu}|r|), \quad (23)$$

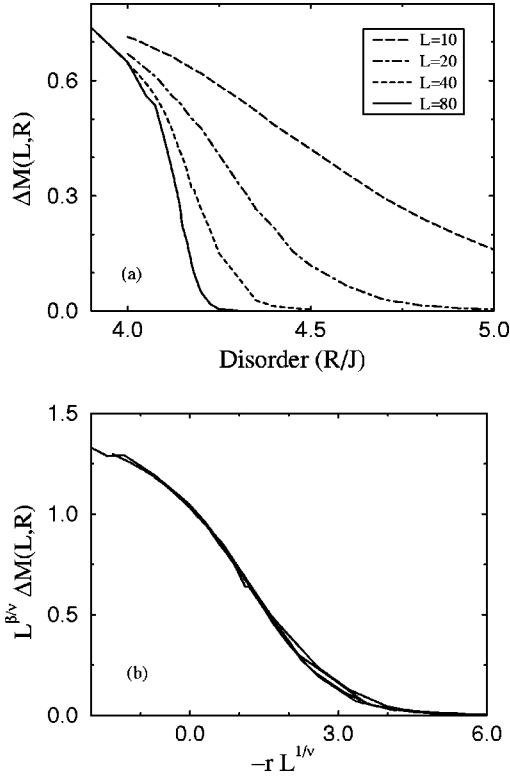


FIG. 11. Jump in the magnetization, in four dimensions. (a) Change in the magnetization due to the spanning avalanches in four dimensions, for several linear sizes L , as a function of the disorder R . (b) Scaling collapse of the curves in (a) using $r = (R_c - R)/R$. The exponents are $1/\nu = 1.12$ and $\beta/\nu = 0.19$, and the critical disorder is $R_c = 4.1$.

where $\Delta\mathcal{M}_\pm$ is a universal scaling function. [The parameter B here, Eq. (5), is unimportant²² because ΔM is measured at $h' = 0$.] Defining a new universal scaling function $\Delta\tilde{\mathcal{M}}_\pm$,

$$\Delta\mathcal{M}_\pm(L^{1/\nu}|r|) \equiv (L^{1/\nu}|r|)^{-\beta} \Delta\tilde{\mathcal{M}}_\pm(L^{1/\nu}|r|), \quad (24)$$

we obtain the scaling form

$$\Delta M(L,R) \sim L^{-\beta/\nu} \Delta\tilde{\mathcal{M}}_\pm(L^{1/\nu}|r|). \quad (25)$$

Figures 11(a) and 11(b) show the change in the magnetization due to the spanning avalanches in four dimensions, and a scaling collapse of that data (similar results exist in three and five dimensions). Notice that as the system size increases, the curves approach the $|r|^\beta$ behavior. The exponents $1/\nu$ and β/ν are extracted from scaling collapses [Fig. 11(b)] and extrapolated to R_c .²² The value of β is calculated from β/ν and the knowledge of ν , and is the value used for collapses of the magnetization curves (discussed earlier).

F. Moments of the avalanche size distribution

The second moment of the integrated avalanche size distribution has a finite-size scaling form

$$\langle S^2 \rangle_{int} \sim L^{-(\tau + \sigma\beta\delta - 3)/\sigma\nu} \tilde{\mathcal{S}}_\pm^{(2)}(L^{1/\nu}|r|), \quad (26)$$

where L is the linear size of the system, r is the reduced disorder, $\tilde{\mathcal{S}}_\pm^{(2)}$ is the scaling function, and ν is the correlation

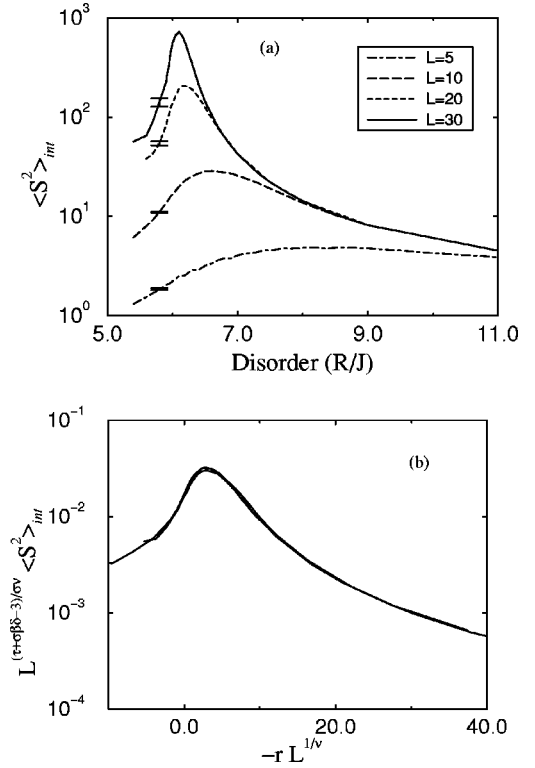


FIG. 12. Second moments. (a) Second moments of the avalanche size distribution integrated over the field H , in five dimensions. Error bars are largest for smaller disorders (shown on the curves). The curves have between 24 and 50 points, and the value of the second moment for each disorder is averaged over 3 to 100 different random field configurations. (b) Scaling collapse of the $L = 10, 20$, and 30 curves from (a) using $r = (R_c - R)/R$. The exponents are $1/\nu = 1.47$ and $\rho = -(\tau + \sigma\beta\delta - 3)/\sigma\nu = 2.95$, and the critical disorder is $R_c = 5.96$.

length exponent. We can similarly define the third and fourth moment, with the exponent $-(\tau + \sigma\beta\delta - 3)/\sigma\nu$ replaced by $-(\tau + \sigma\beta\delta - 4)/\sigma\nu$ and $-(\tau + \sigma\beta\delta - 5)/\sigma\nu$, respectively. Figures 12(a) and 12(b) show the second moments data in five dimensions for sizes $L = 5, 10, 20$, and 30 , and a collapse (again, results in three and four dimensions are similar and we have chosen to show the curves in five dimensions for variety). The curves are normalized by the average avalanche size integrated over all fields H : $\int_{-\infty}^{\infty} \int_1^{\infty} SD(S,R,H,L) dS dH$. The spanning avalanches are not included in the calculation of the moments. We omit the $L = 5$ curve from the collapse; it doesn't collapse with the others well, presumably because of subdominant finite size effects. The exponents for the third and fourth moment can be calculated from those of the second moment, and we find that they agree with the values obtained from their respective collapses.

G. Avalanche time measurement

The exponents we have measured so far are static scaling exponents: they do not depend on the dynamics of the model. If we measure the time an avalanche takes to occur, we are making a dynamical measurement. The time measurement in the numerical simulation is done by increasing the time clock by one for each shell of spins in the avalanche. That is, we

implement time as a synchronous dynamics, where in each time step all unstable spins from the previous step are flipped. The scaling relation between the time t it takes an avalanche to occur and the linear size ξ of the avalanche defines the critical exponent z :^{36,37}

$$t \sim \xi^z. \quad (27)$$

The exponent z is known as the dynamical critical exponent. Equation (27) gives the scaling for the time it takes for a spin to “feel” the effect of another a distance ξ away. Since the correlation length ξ scales like $r^{-\nu}$ close to the critical disorder, and the characteristic size S as $r^{-1/\sigma}$, the time t then scales with avalanche size as

$$t \sim S^{\sigma\nu z}. \quad (28)$$

In our simulation, we measure the distribution of times for each avalanche size S . The distribution of times $D_i(S, R, H, t)$ for an avalanche of size S close to the critical field H_c and critical disorder R_c is

$$D_i(S, R, H, t) \sim S^{-q} \bar{D}_{\pm}^{(i)}(S^{\sigma}|r|, h/|r|^{\beta\delta}, t/S^{\sigma\nu z}), \quad (29)$$

where $q = \tau + \sigma\nu z$, and is defined such that

$$\int_{-\infty}^{+\infty} \int_1^{\infty} D_i(S, R, H, t) dH dt = S^{-(\tau + \sigma\beta\delta)} \bar{D}_{\pm}^{(int)}(S^{\sigma}|r|), \quad (30)$$

where $\bar{D}_{\pm}^{(int)}$ was defined in the integrated avalanche size distribution section. The avalanche time distribution integrated over the field H , at the critical disorder ($r=0$) is

$$D_i^{(int)}(S, t) \sim t^{-(\tau + \sigma\beta\delta + \sigma\nu z)/\sigma\nu z} \bar{D}_i^{(int)}(t/S^{\sigma\nu z}), \quad (31)$$

which is obtained from Eq. (29) (Ref. 22).

Figures 13(a) and 13(b) show the avalanche time distribution integrated over the field H for different avalanche sizes, and a collapse of these curves using the above scaling form, for a 800^3 system at $R=2.260$ (just above the range where spanning avalanches occur). The data are saved in logarithmic size bins, each about 1.2 times larger than the previous one. The time is also measured logarithmically (next bin is 1.1 times larger than the previous one). The extracted value for z in three dimensions is 1.68 ± 0.07 . The results for other dimensions are listed in Table I.

V. COMPARISON WITH THE ANALYTICAL RESULTS

Here we compare the simulation results with the renormalization-group analysis of the same system.^{14,15} According to the renormalization group the upper critical dimension (UCD), at and above which the critical exponents are equal to the mean-field values, is 6. Close to the UCD, it is possible to do a $6 - \epsilon$ expansion, and obtain estimates for the critical exponents and the magnetization scaling function, which can then be compared with our numerical results.

The study of the $6 - \epsilon$ expansion for the equilibrium, thermal random-field Ising model has a contentious history and remains controversial. Much of this controversy is relevant also to our model, and a brief summary would seem necessary despite the numerical focus of this paper. Details and references can be found in Ref. 14. The ϵ expansion for our

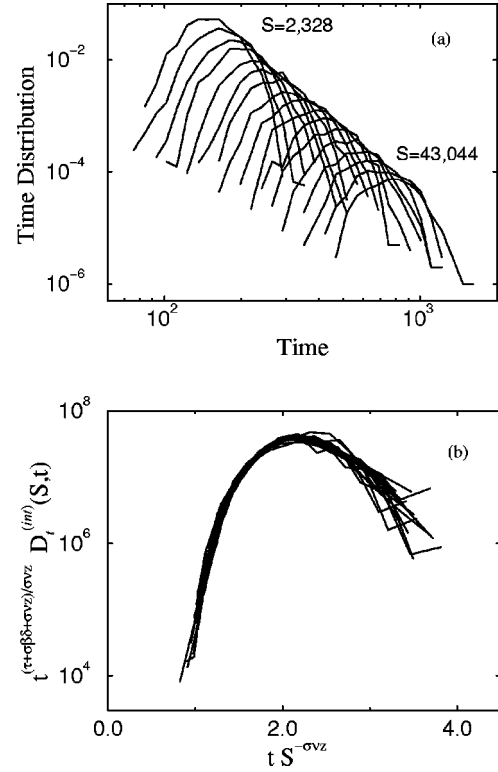


FIG. 13. (a) Avalanche time distribution curves in three dimensions, for avalanche size bins from about 2000 to 40 000 spins (from upper left to lower right corner). The system size is 800^3 at $R=2.26$. The curves are from only one random-field configuration. (b) Scaling collapse of curves in (a). The values of the exponents are $\sigma\nu z=0.57$ and $(\tau + \sigma\beta\delta + \sigma\nu z)/\sigma\nu z=4.0$.

hysteresis model and the thermal random-field model in $6 - \epsilon$ can be mapped to all orders onto the ϵ expansion of the pure, thermal Ising model in $4 - \epsilon$. The critical exponents in lower dimensions, and in particular the lower critical dimension, do not map onto one another. Either there is a nonanalytic correction with a zero power series like $\exp(-1/\epsilon)$, or perhaps the derivation of the ϵ expansion is flawed. Since the ϵ expansion works rather well for our model (details below), and since the argued flaws in the calculational approach for the thermal model did not appear to apply to our method of calculation, we suggested^{14,15} that the discrepancy between pure and disordered exponents (lack of dimensional reduction) was possibly due to a nonanalytic term, leaving the ϵ expansion valid, but incomplete. (This conclusion was compatible with the observation of replica symmetry breaking in the $1/N$ expansions for these models: the bounds in Ref. 38 when examined near six dimensions are compatible with a nonanalytic correction.) Recent work³⁹ has suggested a far more tangible cause for the failure of the theory for the thermal random-field Ising model: a divergence in certain naively irrelevant diagrams which occur both in replica theory and in an unconventional limit of the dynamical theory. We are corresponding with these authors discussing details of their calculations. Pending resolution of these knotty analytical questions, we compare our results to this controversial expansion in $6 - \epsilon$ dimensions.

Figure 14 shows the numerical and analytical results for five of the critical exponents obtained in dimensions 2 to 6 (in six dimensions, the values are the mean-field ones). The

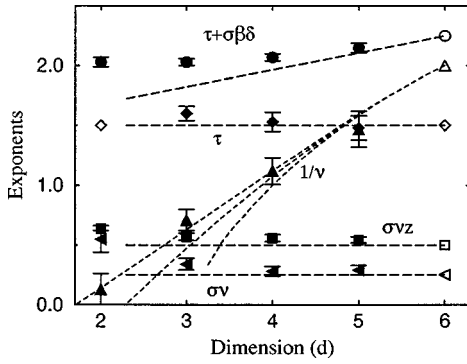


FIG. 14. Comparison between the critical exponents from the simulation and the ϵ expansion. Numerical values (filled symbols) of the exponents $\tau + \sigma\beta\delta$, τ , $1/\nu$, $\sigma\nu z$, and $\sigma\nu$ (circles, diamond, triangles up, squares, and triangle left) in two, three, four, and five dimensions. The empty symbols are values for these exponents in mean field (dimension 6). Exponents in two dimensions are discussed elsewhere.^{12,22,23} Note that the value of τ is two-dimensional conjectured value.¹² We have simulated sizes up to $30\,000^2$, 1000^3 , 80^4 , and 50^5 , where for 320^3 , for example, more than 700 different random-field configurations were measured. The long-dashed lines are the ϵ expansions to first order for the exponents $\tau + \sigma\beta\delta$, τ , $\sigma\nu z$, and $\sigma\nu$. The short-dashed lines are Borel sums⁴⁰ for $1/\nu$, as discussed in Ref. 12. The lowest is the variable-pole Borel sum from LeGuillou *et al.*,⁴⁰ the middle uses the method of Vladimirov *et al.* to fifth order, and the upper uses the method of LeGuillou *et al.*, but without the pole and with the correct fifth-order term. The error bars denote systematic errors in finding the exponents from extrapolation of the values obtained from collapses of curves at different disorders R . Statistical errors are smaller.

other exponents can be obtained from scaling relations.¹⁴ The exponent values in Fig. 14 are obtained by extrapolating the results of scaling collapses to either $R \rightarrow R_c$ or $1/L \rightarrow 0$ (see Ref. 22). The long-dashed lines are the ϵ expansions to first order for $\tau + \sigma\beta\delta$, τ , $\sigma\nu z$, and $\sigma\nu$. The three short-dashed lines¹⁴ are Borel sums⁴⁰ for $1/\nu$. Notice that the numerical values converge nicely to the mean-field predictions, as the dimension approaches 6, and that the agreement between the numerical values and the ϵ expansion is quite impressive.

The ϵ expansion can be an even more powerful tool if it can predict the scaling functions. This has been done for the magnetization scaling function of the pure Ising model in $4 - \epsilon$ dimensions.^{42,41} Since, as discussed above, the ϵ expansion for our model is the same as the one for the *equilibrium* RFIM,¹⁴ and the latter has been mapped to all orders in ϵ to the corresponding expansion of the regular Ising model in two lower dimensions,^{14,43,44} we can use the results obtained in Refs. 42 and 41. This is done in Fig. 15, which shows the comparison between the dM/dH curves obtained in five dimensions and the predicted scaling function for dM/dH , to third order in ϵ , where $\epsilon = 1$ in five dimensions (see Ref. 41). As we see, the agreement is very good in the scaling region (close to the peaks).

VI. SUMMARY

We have used the zero-temperature random-field Ising model, with a Gaussian distribution of random fields, to

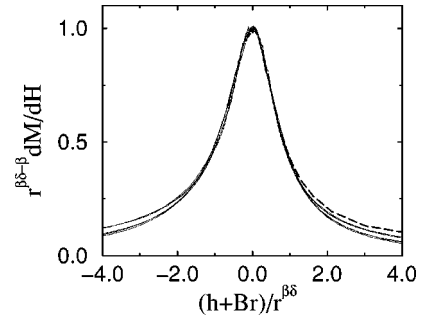


FIG. 15. Comparison between simulated dM/dH curves in five dimensions, and the dM/dH curve obtained from the ϵ expansion. The thick dashed line shows the prediction of the ϵ expansion to third order in ϵ for the slope of the magnetization curve dM/dH in five dimensions. The theoretical curve is a parametric form⁴¹ taken from the analysis of the ordinary, pure, thermal Ising model in three dimensions.¹⁵ The six simulation curves (thin lines) are for a system of 30^5 spins at disorders 7.0, 7.3, and 7.5 ($R_c = 5.96$ in five dimensions), and for a system of 50^5 spins at disorders 6.3, 6.4, and 6.5. The latter curves are closer to the theoretical dashed line. All the curves have been stretched/shrunk in the horizontal and vertical direction and shifted horizontally to lie on each other.

model a random system that exhibits hysteresis. We found that the model has a transition in the shape of the hysteresis loop, and that the transition is critical. The tunable parameters are the amount of disorder R and the external magnetic field H . The transition is marked by the appearance of an infinite avalanche in the thermodynamic system. Near the critical point, (R_c, H_c) , the scaling region is quite large: the system can exhibit power-law behavior for several decades, and still not be near the critical transition. This is important to keep in mind whenever experimental data are analyzed: decades of scaling need not imply self-organized criticality.

We have extracted critical exponents for the magnetization, the avalanche size distribution (integrated over the field and binned in the field), the moments of the avalanche size distribution, the avalanche correlation, the number of spanning avalanches, and the distribution of times for different avalanche sizes. These values are listed in Table I, and were obtained as an average of the extrapolation results (to $R \rightarrow R_c$ or $L \rightarrow \infty$) from several measurements.²² As shown earlier, the numerical results compare well with the ϵ expansion.^{14,15} Comparisons to experimental Barkhausen noise measurements¹² are very encouraging.

ACKNOWLEDGMENTS

We acknowledge the support of DOE Grant No. DE-FG02-88-ER45364 and NSF Grant No. DMR-9805422. We thank Matt Kuntz for noticing and fixing the differences between our analytical and numerical avalanche correlation functions. We would like to thank Sivan Kartha, Bruce Roberts, M. E. J. Newman, J. A. Krumhansl, J. Souletie, and M. O. Robbins for helpful conversations. This work was conducted partly on the SP1 and SP2 at the Cornell Theory Center (funded in part by the National Science Foundation, by New York State, and by IBM), and partly on IBM 560 workstations and an IBM J30 SMP system (both donated by IBM). Further pedagogical information is available at <http://www.lassp.cornell.edu/sethna/hysteresis/> and <http://SimScience.org/crackling/>.

- *Present address: McKinsey & Company, 555 California Street, Suite 4700, San Francisco, CA 94104.
- †Present address: Department of Physics, University of Illinois, Urbana, IL 51801.
- ¹J. D. Shore, M. Holzer, and J. P. Sethna, *Phys. Rev. B* **46**, 11 376 (1992); J. D. Shore and J. P. Sethna, *ibid.* **43**, 3782 (1991); T. Riste and D. Sherrington, in *Phase Transitions and Relaxation in Systems with Competing Energy Scales*, Vol. 415 of NATO Advanced Study Institute, Series C: Mathematical and Physical Sciences, edited by T. Riste and D. Sherrington (Kluwer Academic Publishers, Dordrecht, 1993), and references therein; M. Mézard, G. Parisi, and M. A. Virasoro, *Spin Glass Theory and Beyond* (World Scientific, Singapore, 1987), and references therein; K. H. Fischer and J. A. Hertz, *Spin Glasses* (Cambridge University Press, Cambridge, 1993), and references therein; G. Grinstein and J. F. Fernandez, *Phys. Rev. B* **29**, 6389 (1984); J. Villain, *Phys. Rev. Lett.* **52**, 1543 (1984); D. S. Fisher, *ibid.* **56**, 416 (1986).
 - ²D. Jiles, *Introduction to Magnetism and Magnetic Materials* (Chapman and Hall, New York, 1991).
 - ³J. C. McClure, Jr. and K. Schröder, *Crit. Rev. Solid State Sci.* **6**, 45 (1976).
 - ⁴K. P. O'Brien and M. B. Weissman, *Phys. Rev. E* **50**, 3446 (1994), and references therein; *Phys. Rev. A* **46**, R4475 (1992); U. Lieneweg and W. Grosse-Nobis, *Int. J. Magn.* **3**, 11 (1972); Djordje Spasojević, Srdjan Bukvić, Sava Milošević, and H. Eugene Stanley, *Phys. Rev. E* **54**, 2531 (1996).
 - ⁵J. S. Urbach, R. C. Madison, and J. T. Markert, *Phys. Rev. Lett.* **75**, 276 (1995).
 - ⁶P. J. Cote and L. V. Meisel, *Phys. Rev. Lett.* **67**, 1334 (1991); L. V. Meisel and P. J. Cote, *Phys. Rev. B* **46**, 10 822 (1992).
 - ⁷P. Bak, C. Tang, and K. Wiesenfeld, *Phys. Rev. Lett.* **59**, 381 (1987); *Phys. Rev. A* **38**, 364 (1988).
 - ⁸S. Field, J. Witt, and F. Nori, *Phys. Rev. Lett.* **74**, 1206 (1995).
 - ⁹W. Wu and P. W. Adams, *Phys. Rev. Lett.* **74**, 610 (1995).
 - ¹⁰M. P. Lilly, P. T. Finley, and R. B. Hallock, *Phys. Rev. Lett.* **71**, 4186 (1993).
 - ¹¹A. Berger (unpublished).
 - ¹²O. Perković, K. A. Dahmen, and J. P. Sethna, *Phys. Rev. Lett.* **75**, 4528 (1995).
 - ¹³J. P. Sethna, K. A. Dahmen, S. Kartha, J. A. Krumhansl, B. W. Roberts, and J. D. Shore, *Phys. Rev. Lett.* **70**, 3347 (1993).
 - ¹⁴Karin A. Dahmen and James P. Sethna, *Phys. Rev. B* **53**, 14 872 (1996); K. A. Dahmen, Ph.D. thesis, Cornell University, 1995.
 - ¹⁵K. A. Dahmen and J. P. Sethna, *Phys. Rev. Lett.* **71**, 3222 (1993).
 - ¹⁶Hong Ji and Mark O. Robbins, *Phys. Rev. B* **46**, 14 519 (1992), and references therein. Ji and Robbins initiated the study of this particular model, except that they use it to study the closely related interface depinning problem (which does not allow avalanches to start except next to existing flipped spins).
 - ¹⁷O. Narayan and D. S. Fisher, *Phys. Rev. Lett.* **68**, 3615 (1992); *Phys. Rev. B* **46**, 11 520 (1992); D. Ertas and M. Kardar, *Phys. Rev. E* **49**, R2532 (1994); C. Myers and J. P. Sethna, *Phys. Rev. B* **47**, 11 171 (1993); **47**, 11 194 (1993).
 - ¹⁸T. Nattermann, S. Stepanow, L. H. Tang, and H. Leschhorn, *J. Phys. II* **2**, 1483 (1992); O. Narayan and D. S. Fisher, *Phys. Rev. B* **48**, 7030 (1993).
 - ¹⁹J.-G. Zhu and H. Neal Bertram, *J. Appl. Phys.* **69**, 4709 (1991), studied a hexagonal two-dimensional model with in-plane magnetization, ferromagnetic bonds with the four neighbors along the field direction, and antiferromagnetic (or missing) bonds with the two neighbors perpendicular to the field.
 - ²⁰C. M. Coram, A. E. Jacobs, N. Heinig, and K. B. Winterbon, *Phys. Rev. B* **40**, 6992 (1989).
 - ²¹E. Vives, J. Goicoechea, J. Ortín, and A. Planes, *Phys. Rev. E* **52**, R5 (1995); E. Vives and A. Planes, *Phys. Rev. B* **50**, 3839 (1994). A comparison between our simulation and their results show that the three-dimensional results agree quite nicely. However, in two dimensions, there are large differences, which we believe occur because of the small system sizes used by the authors for their simulation (only up to $L=100$, but they reported their results first). We have seen that our results are very size dependent. We would expect for a system of $L=100$ spins to find a critical disorder $R_c=0.75$, as was found by these authors; however, we find after increasing the system size that the critical disorder is 0.54 or lower (Refs. 22 and 23). These authors also explore the zero temperature random bond Ising model, which they show also exhibits a critical transition in the shape of the hysteresis loop, where the mean bond strength is analogous to our disorder R . They give numerical evidence that the random bond Ising model is in the same universality class as our random-field model. We argue elsewhere on symmetry grounds that this is likely the case (Ref. 14), and that the experimentally more relevant random-anisotropy model is also likely described by our critical point.
 - ²²O. Perković, K. A. Dahmen, and J. P. Sethna, cond-mat/9609072 (unpublished).
 - ²³M. C. Kuntz, O. Perković, and J. P. Sethna (unpublished).
 - ²⁴M. C. Kuntz, O. Perković, K. A. Dahmen, B. W. Roberts, and J. P. Sethna, cond-mat/9809122; code and documentation available at <http://www.lassp.cornell.edu/sethna/hysteresis/code>.
 - ²⁵D. Dhar, P. Shukla, and J. P. Sethna, *J. Phys. A* **30**, 5259 (1997).
 - ²⁶K. G. Wilson, *Phys. Rev. B* **4**, 3174 (1971); **4**, 3184 (1971); K. G. Wilson and M. E. Fisher, *Phys. Rev. Lett.* **28**, 240 (1972); K. G. Wilson and J. Kogut, *Phys. Rep., Phys. Lett.* **C12**, 75 (1974); J. M. Yeomans, *Statistical Mechanics of Phase Transitions* (Clarendon Press, Oxford, 1992); M. Plischke and B. Bergersen, *Equilibrium Statistical Physics* (Prentice Hall, Englewood Cliffs, NJ, 1989); S. Ma, *Modern Theory of Critical Phenomena* (Benjamin, Reading, MA, 1976); M. E. Fisher, in *Critical Phenomena*, Lecture Notes in Physics Vol. 186, edited by F. J. W. Hahne (Springer-Verlag, Berlin, 1983).
 - ²⁷S. Wiseman and E. Domany, *Phys. Rev. E* **52**, 3469 (1995); A. Aharony and A. B. Harris, *Phys. Rev. Lett.* **77**, 3700 (1996).
 - ²⁸S. Wiseman and E. Domany, *Phys. Rev. Lett.* **81**, 22 (1998); *Phys. Rev. E* **58**, 2938, Part A (1998).
 - ²⁹F. Pázmándi, R. T. Scalettar, and G. T. Zimányi, *Phys. Rev. Lett.* **79**, 5130 (1997).
 - ³⁰C. R. Myers and J. P. Sethna, *Phys. Rev. B* **47**, 11 194 (1993).
 - ³¹In three and four dimensions, below the critical field H_c , we have not found any spanning avalanches. In five dimensions, spanning avalanches appeared below the critical field $H_c = 1.175$. We believe this is due to the small system size (30^5) used for the five-dimensional simulation. We, however, do not expect substantial corrections to the exponents derived from that data.
 - ³²The divergence in the number of spanning avalanches near R_c and the association with hyperscaling was originally discussed in our response to a comment by A. Maritan, M. Cieplak, M. R. Swift, and J. Banavar, *Phys. Rev. Lett.* **72**, 946 (1994); J. P. Sethna, K. A. Dahmen, S. Kartha, J. A. Krumhansl, O. Perković, B. W. Roberts, and J. D. Shore, *ibid.* **72**, 947 (1994).

- ³³L. de Arcangelis, *J. Phys. A* **20**, 3057 (1987); A. Coniglio, *Springer Proc. Phys.* **5**, 84 (1985).
- ³⁴D. Stauffer and A. Aharony, *Introduction to Percolation Theory*, revised 2nd ed. (Taylor & Francis, London, 1992).
- ³⁵For a good introduction on static scaling and finite size scaling, see N. Goldenfeld, *Lectures on Phase Transition and the Renormalization Group* (Addison Wesley, Reading, MA, 1992); M. N. Barber, in *Phase Transitions and Critical Phenomena*, Vol. 8, edited by C. Domb and J. L. Lebowitz (Academic Press, New York, 1983).
- ³⁶P. C. Hohenberg and B. I. Halperin, *Rev. Mod. Phys.* **49**, 435 (1977).
- ³⁷J. J. Binney, N. J. Dowrick, A. J. Fisher, and M. E. J. Newman, *The Theory of Critical Phenomena* (Clarendon Press, Oxford, 1992); S. Ma, *Modern Theory of Critical Phenomena* (Benjamin, Reading, MA, 1976).
- ³⁸M. Mezard and P. J. Young, *Europhys. Lett.* **18**, 653 (1992).
- ³⁹E. Brézin and C. De Dominicis, *Europhys. Lett.* **44**, 13 (1998); cond-mat/9807113 (unpublished).
- ⁴⁰H. Kleinert, J. Neu, V. Schulte-Frohlinde, K. G. Chetyrkin, and S. A. Larin [*Phys. Lett. B* **272**, 39 (1991); and erratum in **319**, 545 (1993)] provide the expansion for the pure, equilibrium Ising exponents to fifth order in $\epsilon=4-d$. A. A. Vladimirov, D. I. Kazakov, and O. V. Tarasov [*Sov. Phys. JETP* **50**, 521 (1979), and references therein] introduce a Borel resummation method with one parameter, which is varied to accelerate convergence. J. C. LeGuillou and J. Zinn-Justin [*Phys. Rev. B* **21**, 3976 (1980)] do a coordinate transformation with a pole at $\epsilon=3$, and later [*J. Phys. (France) Lett.* **46**, L137 (1985); and *J. Phys. (France)* **48**, 19 (1987)] make the placement of the pole a variable parameter (leading to a total of four real acceleration parameters for a fifth-order expansion!). Unfortunately, LeGuillou *et al.* used a form for the fifth-order term which turned out to be incorrect (Kleinert, above). The ϵ expansion is an asymptotic series, which need not determine a unique underlying function [J. Zinn-Justin *Quantum Field Theory and Critical Phenomena*, 2nd edition (Clarendon Press, Oxford, 1993)]. Our model likely has nonperturbative corrections [as did the equilibrium, thermal random-field Ising model (Ref. 44)].
- ⁴¹J. Zinn-Justin, *Quantum Field Theory and Critical Phenomena*, 2nd ed. (Clarendon Press, Oxford, 1993).
- ⁴²E. Brézin, D. J. Wallace, and K. G. Wilson, *Phys. Rev. Lett.* **29**, 591 (1972); *Phys. Rev. B* **7**, 232 (1973); G. M. Avdeeva and A. A. Midgal, *JETP Lett.* **16**, 178 (1972); D. J. Wallace and R. P. K. Zia, *Phys. Lett. A* **46**, 261 (1973); D. J. Wallace and R. P. K. Zia, *J. Phys. C* **7**, 3480 (1974); C. Domb and M. S. Green, *Phase Transitions and Critical Phenomena* (Academic Press, New York, 1976), Vol. 6, Sec. 5, and references therein.
- ⁴³A. Aharony, Y. Imry, and S. K. Ma, *Phys. Rev. Lett.* **37**, 1364 (1976); G. Parisi and N. Sourlas, *ibid.* **43**, 744 (1979).
- ⁴⁴G. Parisi, in *Recent Advances in Field Theory and Statistical Mechanics* lectures given at the 1982 Les Houches Summer School XXXIX (North-Holland, Amsterdam, 1983), and references therein.